AD-A032 449 PENNSYLVANIA UNIV PHILADELPHIA DEPT OF CHEMICAL AND --ETC F/G 11/6
HYDROGEN DIFFUSION AND EMBRITTLEMENT IN 4340 STEEL.(U)
JUN 76 L NANIS, T K NAMBOODHIRI N00014-67-A-0216-0004
UNCLASSIFIED UPH2-005 NL

1 OF 1
ADA032449

END

DATE
FILMED
1 -77

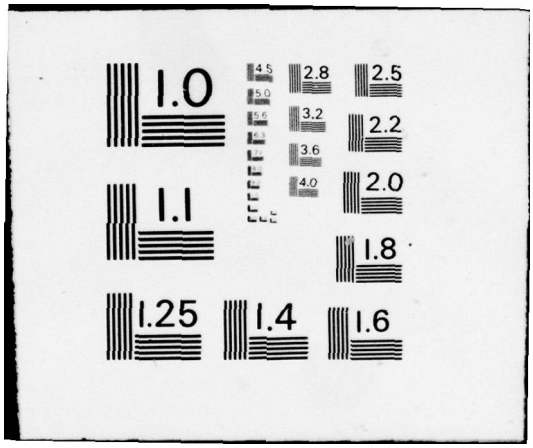
1.0
1.1
1.25
1.4
1.6
1.8
2.0
2.2
2.5
2.8
3.2
3.6
4.0
4.5
5.0
5.6

(12) PP

(6)

# HYDROGEN DIFFUSION AND EMBRITTLEMENT IN 4340 STEEL.

by

(10) Leonard/Nanis
and
T.K. Govindan/Namboodhiri

(11) Jun 76

(12) 27P.

(9) (14) FINAL REPORT. UPH2-005
JUNE 1976

NR 036-077
OFFICE OF NAVAL RESEARCH

Fundamental Corrosion Studies:
Hydrogen Embrittlement

Contract N00014-67-A-0216-0004
(15)





Senior Investigator

Dr. Leonard Nanis
Department of Chemical and Biochemical Engineering
College of Engineering and Applied Science
University of Pennsylvania
Philadelphia, Pennsylvania 19174

Table of Contents

# HYDROGEN DIFFUSION AND EMBRITTLEMENT IN 4340 STEEL

T.K. Govindan Namboodhiri and Leonard Nanis
Department of Chemical and Biochemical Engineering
College of Engineering and Applied Science
University of Pennsylvania
Philadelphia, Pennsylvania 19174

## ABSTRACT

The sensitive electrochemical permeation technique was used in conjunction with scanning electron microscopy and tensile loading to determine ~~(i)~~ hydrogen diffusivity and solubility, ~~(ii)~~ effect of plastic deformation on the above parameters, and ~~(iii)~~ structural features and kinetics of hydrogen embrittlement, in 4340 steel. The salient results are: (a) time to failure is directly proportional to the square of the distance through which hydrogen must travel in order to reach a stressed region at the root of a notch, clearly indicating the role played by diffusion; (b) the critical hydrogen concentration for embrittlement of quenched and tempered 4340 steel is on the order of 0.5 ppm. Also of interest: (c) small amounts of plastic deformation of annealed 4340 result in drastic increases in hydrogen solubility and proportional reductions in diffusivity; (d) hydrogen diffusivity of quenched and tempered 4340 is about 25 times smaller than that of annealed material; (e) in quenched and tempered 4340, plastic yielding precedes hydrogen embrittlement; and (f) the ductility of annealed 4340 is reduced by 50% when fully charged with hydrogen.

# HYDROGEN DIFFUSION AND EMBRITTLEMENT IN 4340 STEEL

## 1. INTRODUCTION

1.1 The focus of all of the work performed on contract NR 036-077 from its initiation in 1969 to its termination in 1973 was the controlled transient placement of hydrogen in stressed steel. Whereas hydrogen is conventionally charged in an attempt to produce a uniform concentration throughout a test specimen, this project has favored an approach of precise definition of electrochemical parameters to permit precise control of hydrogen profile as a function of both position and time. Much effort was devoted to unravelling mysteries of hydrogen permeation behavior for well-studied Armco iron in preparation for application of the electrochemical permeation method to 4340 steel prepared with a variety of specific strength levels. While this contract was terminated before the carefully planned sequence could be fully accomplished, sufficient progress was made to offer totally new insights into the mechanism of H.E. The ability to direct an amount of dissolved hydrogen into material with a pre-determined stress pattern when and where it is desired is a powerful tool still awaiting fullest exploitation. When the main body of H.E. workers learn to combine metallurgy and electrochemistry as we have done, the work of this ONR contract will ultimately be recognized as having charted the unknown to enable hydrogen embrittlement to be explained and controlled.

1.2 It is well-known (1) that hydrogen produces severe embrittlement in high strength steels. Stress corrosion cracking of all martensitic steels is now thought (2) to be invariably associated with hydrogen embrittlement. The ability of hydrogen to promote catastrophic embrittlement in steel pipes in the hydrogen sulphide atmosphere of sour gas wells producing natural gas has been a source of much worry in that industry for years (3). The severity of problems resulting from hydrogen embrittlement has generated a considerable amount of research aimed at discovering the causes and prevention of this phenomenon. These studies have brought out the following salient features of hydrogen embrittlement in steels:

1.2.1 Only low hydrogen concentrations of about few parts per million are sufficient to embrittle high strength steels. However, no embrittlement takes place when the hydrogen concentration is below a critical minimum value (4).

1.2.2 Dissolved hydrogen does not alter significantly either the shape of the stress-strain curve or the yield stress of the material (5).

1.2.3 In contrast to conventional embrittlements, hydrogen embrittlement is inversely proportional to strain rate, i.e. hydrogen embrittlement is most pronounced at very low strain rates or at static loading conditions. Delayed failure or static fatigue is a unique feature of hydrogen embrittlement where the material fails under the action of a sustained load well below that needed to initiate plastic flow under normal conditions (5).

1.2.4 Crack propagation during hydrogen induced failure has an incubation period and proceeds discontinuously.

1.3 Based on the experimental observations listed in Sec. 1.2.1-1.2.4, it has been postulated (7) that hydrogen embrittlement is induced by the stress-induced diffusion of hydrogen to regions of high stress concentrations where it reduces the maximum cohesive resistive force of the lattice. Existing or freshly created cracks propagate when the local tensile elastic stress normal to the crack equals the local maximum cohesive force.

AISI 4340 Steel is a widely-used high-strength low-alloy steel and it has been found to be susceptible to hydrogen embrittlement (5). Delayed failure characteristics of this steel are well established (4,5,6). However, until now no accurate measurements of hydrogen diffusivity and solubility in the material have been reported. This final report deals with the measurement of these important parameters in 4340 heat treated to various strength levels. By the use of electrochemically controlled position-time profiles, the critical minimum hydrogen concentration needed for embrittlement is calculated and the role of hydrogen diffusion in embrittlement is clearly brought out. Fractographic features of hydrogen induced failure in this steel are also correlated with controlled hydrogen profiles.

## 2. EXPERIMENTAL

2.1 Commercial aircraft quality 4340 steel was used for this investigation. The materials obtained in the form of sheet 12x2x0.063 in. had the following chemical composition (wt %):

C - 0.39, Mn - 0.63, Ni - 1.81, Cr - 0.81, Mo - 0.24, Cu - 0.14, Si - 0.30, S - 0.023, P - 0.009, Fe - balance.

As - received strips were cold rolled to thicknesses in the range of 0.015 to 0.03 in. This material was then either annealed at 650°C (1200°F) for 10 hours and slowly cooled or austenitised, oil quenched, and tempered at lower temperatures. Austenitising was done, either at 800°C (1475°F) or 870°C (1600°F) for one hour and then oil quenched. Quenched steel was then tempered at 260°C (450°F) or 350°C (660°F) for two hours.

2.2 The highly sensitive electrochemical permeation technique (9) was used to determine hydrogen diffusivity and solubility in the steel. In this method, a thin metallic membrane is cathodically charged with hydrogen on one side while the other side is maintained at a constant potential sufficiently anodic to oxidize all of the hydrogen diffusing out to the potentiostated side. The anodic current, measured between the metallic membrane and a platinum counter electrode, is a direct measure of the rate at which hydrogen diffuses out at the anodic side. From the transient anodic permeation current resulting from the starting or interruption of cathodic hydrogen charging, the hydrogen diffusion coefficient of the metallic membrane can be calculated. From the steady state permeation current at any particular charging condition, the corresponding hydrogen solubility in the metal may be evaluated. The details of this technique may be found elsewhere (10,11).

2.3 Permeation experiments were carried out using an all-plastic permeation cell (12). The anodic surface of the steel membrane was always protected by a thin layer of palladium obtained by electroless deposition. The anodic side of the membrane was potentiostated at -330 to -150 mV with respect to a saturated calomel electrode. The anode electrolyte was always 0.2 N NaoH solution. Cathodic charging was done from either 0.2 N NaoH or 0.1 N $H_2SO_4$ electrolytes, using a separate constant current circuit.

Tensile and static fatigue tests were performed on a table model Instron machine. Scanning electron microscopic studies of the fracture surfaces were carried out using a JEOLCO JSM-U3 microscope operated at a voltage of 25 KV.

## 3. RESULTS AND DISCUSSION

### 3.1 Correlation between strength level of 4340 and its hydrogen diffusivity and solubility.

It is known (4) that the susceptibility of 4340 steel to hydrogen embrittlement increases as the strength level of the steel increases. Hence, it is of interest to know how hydrogen diffusivity and solubility in the steel vary with the strength level. Hydrogen permeation experiments were carried out on annealed as well as quenched and tempered steel samples. The results are given in Table 1 where it may be seen that the annealed steel has the highest hydrogen diffusivity and lowest hydrogen solubility. In quenched and tempered samples, the diffusivity is more than one order of magnitude smaller than

in the annealed material. The diffusivity of quenched and tempered steel shows a minor decrease as the strength level increases. The hydrogen solubility of quenched and tempered material is more than an order of magnitude larger than that of annealed material. An increase in solubility as the strength level increases is also shown in Table 1.

It must be pointed out here that hydrogen diffusivity measured by the permeation technique is highly sensitive to structural defects such as dislocations, solute atoms and vacancies, and also to internal defects such as inclusions and microcracks in the metallic membrane. Unless the membrane is free from all of these defects, the measured diffusivity value will be different from the true lattice diffusivity of the metal. Here, 4340 steel in the annealed condition consists of ferrite and connentite in the equilibrium condition and is relatively defect free. Upon quenching from the austenitic field, the steel consists of martensite plates which produces a highly defective internal structure. Tempering of the martensite results (13) in the preciptation of ε-carbide. These carbide precipitates introduce large microstresses within the matrix. These stressed regions, the carbide-martensitic interfaces and the martensitic plate interfaces are possible trapping sites for hydrogen. It has also been pointed out (14) that ε-carbide may dissolve large amounts of hydrogen to form a stoichiometric compound, $Fe_2HC$. Thus, trapping and possible preferential dissolution by ε-carbide could explain the large hydrogen solubilities of quenched

Table 1

Hydrogen permeation characteristics of 4340

Catholyte: 0.2N NaoH
Temperature: 22°C
Charging current density: 3.31 $mA/cm^2$

| Heat treatment | Yield strength | Ultimate tensile strength (Ksi) | Diffusivity $D \times 10^6$ ($cm^2/sec$) | Concentration $C_{Ave} \times 10^7$ mole H/cc |
|---|---|---|---|---|
| 1. Annealed | 72 | 84 | 7.5 | 0.87 |
| 2. Quenched from 1475°F, tempered at 660°F for 2 hrs. | 185 | 219 | 0.24 | 20.9 |
| 3. Quenched from 1600°F, tempered at 450°F for 2 hrs. | 240 | 270 | 0.22 | 36.8 |

and tempered 4340 steel. As the tempering temperature increases, the microstresses associated with the ε-carbide as well as the amount of ε-carbide decreases (15) and this accounts for the reduced hydrogen solubility.

3.2 Effect of hydrogen charging on tensile test results of 4340

Tensile testing of annealed as well as of quenched and tempered steels was carried out on flat sheet specimens. Notched specimens had a semi-circular notch at the middle of the gauge length on one side of the specimen, running completely across the specimen width (shown in the inset of Fig. 1). Since it is known (16) that hydrogen embrittlement is facilitated by slow loading rates, all tensile tests were done at a cross-head speed of 0.02 inch/minute.

3.2.1 Annealed 4340

Unnotched tensile specimens of annealed 4340 were hydrogen charged from both sides using 0.4N $H_2SO_4$ electrolyte. After hydrogen charging the specimens "in-situ" on the testing machine for one hour, specimens were loaded to failure. The procedure was repeated at various charging current densities to reveal the effect of various hydrogen concentrations in the specimen. From the tensile load-elongation curve of this material, it may be seen that dissolved hydrogen has relatively no effect on the elastic region of the curve as well as no effect on the yield strength of the material. All that the hydrogen does is to reduce the elongation at fracture of the material. While the elongation at fracture of uncharged material was about 30%, that of a severely hydrogen charged specimen was reduced to 15.6%.

Fracture surfaces of charged specimens were observed in the scanning electron microscope. The fracture was seen to be completely ductile in nature as evidenced by the presence of dimples resulting from microvoid coalscenee during fracture. This suggests that hydrogen charging does not produce any embrittlement as such in annealed 4340 and that the reduction of ductility from 30% to 15.6% elongation may be a solid solution effect.

3.2.2 Quenched and tempered 4340 steel

Notched tensile specimens of 4340 steel, quenched from 1600°F and tempered at 450°F for 2 hours, were hydrogen charged from both sides using 0.1 N $H_2SO_4$. Stressing started as soon as cathodic charging began and continued until specimens failed. Table 2 shows the results of tensile testing on specimen hydrogen charged at different current densities. While a notched specimen tested in air failed at a stress 1.37 times the yield stress, a notched specimen immersed in 0.1 N $H_2SO_4$ (with zero charging current) fails at 0.60 times the yield stress. Hydrogen charging at increasing current densities steadily decreased the fracture stress. This behavior is clearly indicative of hydrogen embrittlement. Examination of fracture surfaces showed that fracture occurred by separation at prior austenitic grain boundaries. Details of the fractographic behavior of this material will be given in Section 4. These tests clearly showed that hydrogen charging of quenched and tempered 4340 produces severe embrittlement, causing the failure of the material at a fraction of its yield stress. This behavior is quite different

Table 2

Tensile test results for hydrogen charged 4340

Material: Quenched from 1600°F and tempered at 450°F for 2 hours; notched tensile specimen.

Charging conditions: Two sided charging from 0.1N $H_2So_4$; 22°C

| Charging current density ($mA/cm^2$) | Stress at fracture, $\sigma f$ (Ksi) | $\frac{\sigma f}{\sigma yield}$ |
|---|---|---|
| 0 (in air) | 329 | 1.37 |
| 0 (in acid) | 143 | 0.60 |
| 0.25 | 127 | 0.53 |
| 1.24 | 103 | 0.43 |

from that of the annealed 4340 given in Section 3.2.1.

3.2.3 Static fatigue tests on quenched and tempered 4340 steel

Static fatigue or delayed failure tests on hydrogen charged specimens of quenched and tempered 4340 were carried out to bring out the essential role played by diffusion in hydrogen embrittlement and to calculate the critical minimum hydrogen concentration needed to produce embrittlement in this material. The notched specimens were hydrogen charged while on the tensile testing machine, using a simple plastic bottle cell which contained either 0.2 N $N_a$oH or 0.1 N $H_2So_4$ as electrolyte. During these tests, the specimen was charged from the side opposite to the side containing the notion (see Fig. 1). The area exposed to the electrolyte and its position with respect to the notch were controlled by masking the remaining area of the specimen with a non-conducting lacquer. Hydrogen charging and tensile loading were started simultaneously. The cross-head of the testing machine was stopped when the desired stress level was attained. Hydrogen charging was continued until the specimens failed and the time to failure was noted.

3.3 Role of diffusion in hydrogen embrittlement

3.3.1 Displaced exposure study

All proposed theories (7,17-19) of hydrogen embrittlement in steels involve diffusion of hydrogen to the root of an existing notch or to other areas of stress concentration. Even in a membrane having a low uniform concentration of hydrogen, embrittlement can occur provided there are regions of stress concentration in the material. Hydrogen diffuses preferentially to regions of stress concentration under the influence of its

activity gradient (20). Published results (4) have clearly shown that hydrogen embrittlement in steels takes place only when large stress concentrations exist (as at the root of a sharp notch) sufficient to produce an excess hydrogen concentration in their vicinity. This is because of the fact that the lattice solubility of hydrogen in iron or steel is very minute and insufficient to cause embrittlement. This low hydrogen concentration has to be enhanced by stress-assisted diffusion to notch roots to produce the embrittling effect. From all these observations it may be seen that diffusion of hydrogen is an unavoidable step in hydrogen embrittlement. The present static fatigue tests were utilized to get a direct correlation between hydrogen diffusion path and failure time.

A series of static fatigue tests were carried out at a constant applied stress level of 122 KSI and with simultaneous hydrogen charging from the side opposite to the notch using 0.1 N $H_2SO_4$ electrolyte and a constant charging current density of 0.25 $mA/cm^2$. The only variable factor in these tests was the distance through which hydrogen had to diffuse before reaching the notch root. Diffusion distance was increased by relocating the hydrogen charging inlet or window area with respect to the plane of the notch root. The time to failure was noted in each case. Fig. 1 shows a plot of the times to fracture as a function of the square of the diffusion distance. It is seen that failure time increases linearly with $L^2$. This clearly indicates that the fracture time is dependent upon the time for hydrogen diffusion to the root of the notch. Fig. 1 also shows two lines

which correspond to $t=2L^2/D$ and $t=0.06L^2/D$ respectively. From hydrogen diffusion calculations in the case of one sided charging of plane sheets (21), it may be seen that

$$t = \frac{0.06L^2}{D} \qquad \text{Eqn. (1)}$$

denotes a time at which the first presence of diffusing hydrogen can be said to have "arrived" at the distance X=L after having been injected at X=0. Eqn. 1 represents a well used rule of thumb for semi-infinite diffusion from a constant intensity surface source. The numerical result in Eqn. 1 is actually obtained by considering a concentration fraction of 0.01 to have built up at X=L and substituting this fraction into an error function complement solution to the diffusion problem. The choice of $C_{x=L}/C_{x=0}=.01$ is somewhat arbitrary, but because of the nature of the error function, concentration fractions of similar magnitude produce little change in the numerical coefficient of Eqn. 1.

In a similar fashion, it may be assumed that hydrogen does not diffuse out at the boundary X=L so that the concentration steadily increases throughout the region $0<x<L$ following input at X=0, until full charging is obtained throughout. It should be noted that the full charging approach is favored by previous workers, thus denying the opportunity to make full utilization of the dynamic nature of the hydrogen charging process. As with most planar geometry diffusion processes, the time for full (i.e. 99%) charging is roughly approximated as

$$t = 2L^2/D \qquad \text{Eqn. (2)}$$

As shown by the dashed lines in Fig. 1, the fracture time vs. $L^2$ plot falls between the curves given by Eqns. 1 and 2 using a measured diffusivity value for quenched and tempered 4340 of $0.22 \times 10^{-6}$ $cm^2$ sec. From a bit of the heavy line to the data points, the time for fracture may be approximated to the equation

$$t = \frac{0.165L^2}{D} \qquad \text{Eqn. 3}$$

In this displaced entry studies, the hydrogen entered on the left side of specimen as shown in the inset of Fig. 1. The distance L used is actually the distance of closest approach to the root of the notch which starts on the right side. Thus, for the entry strip located exactly opposite the notch root, the distance 0.026 cm serves as a minimum travel distance for hydrogen. The linear distance scale is provided for convenience at the top of Fig. 1.

The important finding of these displaced exposure studies is the fact that the hydrogen induced delayed failure is directly dependent upon diffusion of hydrogen to the vicinity of the root of the notch where maximum stress concentration exists. Even though this fact has been established previously by indirect means (4), this is the first instance of a direct experimental verification.

### 3.3.2 Critical hydrogen concentration

The importance of a critical hydrogen concentration in producing hydrogen embrittlement in steels has been well established (4). Delayed failure studies on hydrogen charged steel (1) have demonstrated the existence of a minimum stress below which no failure occurs. Absence of hydrogen-induced failure below the static fatigue limit has been attributed (4) to the inability of the stress system to produce the needed critical hydrogen concentration by stress-induced diffusion. Using the electrochemical permeation technique and static fatigue testing, an estimation of the critical hydrogen concentration may be made. First, the notch geometry may be ignored as an approximation so that from hydrogen permeation data and a model for hydrogen diffusion from one side into a plane sheet with zero flux at the other side, an estimate of hydrogen concentration at any particular point in the specimen may be made. Henry (21) has made diffusion calculations applicable to plane sheets which give concentration distribution curves across the specimen thickness at various times. Knowing the specimen dimensions, the diffusion distance, L, from the charging side to the notch root plane can be calculated. By assuming no loss of hydrogen at X=L and by using a known value for diffusivity, the failure time may be used to evaluate the dimensionless group $Dt/L^2$ equal to 0.165, as given in Eqn. 3. The concentration versus time for X=L may then be readily evaluated from the well-known planar diffusion concentration profiles calculated

by Henry (21). This gives the hydrogen concentration at the root of the notch as a fraction of the equilibrium concentration at the charging side. This latter concentration can be obtained from permeation studies. However, the notch root concentration thus obtained does not take into account the high stress concentration existing at the notch root.

Oriani (22) has calculated the stress-enhanced concentration of hydrogen in steels using the relationship,

$$\frac{C^{\sigma}}{C^{o}} = \exp \frac{\overline{V}_H \sigma}{3RT} \qquad \text{Eqn. 4}$$

where

$C^{\sigma}$ = solubility at stress $\sigma$, mole/cc

$C^{o}$ = solubility at zero stress, mole/cc

$\overline{V}_H$ = partial molar volume of hydrogen, cc/mole

R = gas constant, $8.31 \times 10^7 \frac{\text{dyne cm}}{\text{mole}^\circ\text{K}}$

T = absolute temperature, °K

$\sigma$ = stress, dyne/cm$^2$

In the present case, the tensile specimens had semi-circular notches resulting in a stress concentration of three times the applied stress at the root of the notches (23). For static fatigue tests, stresses in the range 98 to 128 KSI were applied. Hence, all these specimens developed stresses much higher than the yield stress of the 4340 (240 KSI) at the notch root. This results in some amount of plastic deformation near the notch root. Under such conditions, the maximum stress concentration

will be at the elastic-plastic boundary and the maximum stress at this region will be about 1.35 $\sigma y$ (where $\sigma y$=yield stress)(24). Hence, the maximum tensile stress near the notch root in the static fatigue specimen was of the order of 324 KSI.

The partial molar volume of hydrogen in iron and steel, $\overline{V}_H$, has been determined by various researchers. One of the most recently reported values is that of Subramanian et al.(25) who obtained a value of 1.96 cc/g atom for $\overline{V}_H$ in 4340 steel. Using these values in Eqn. 4, $C^{\sigma}/C^{o}$ was calculated to be 1.81.

Table 3 shows the calculation of critical concentration at the root of the notch at the time of failure for static fatigue tested specimens. The two specimens were hydrogen charged from 0.2N NaoH at 0.125 $mA/cm^2$ and 0.250 $mA/cm^2$ respectively.

The hydrogen concentrations at the charging side of the specimens ($C_o$) were calculated from separate experiments in which the input concentration $C_o$ was correlated with cathodic charging current density. This information is obtained as the steady state is reached in electrochemical permeation studies. Following the transient period, each input current density produces a corresponding permeation current density $J_\infty$, detected by the potentiostat. The concentration at X=0 may be obtained from Eqn. 5 (Fick's first law) as

$$C_o = \frac{J_\infty L}{F} \qquad \text{Eqn. 5}$$

where L = permeation distance, cm; D = diffusion coefficient, $cm^2/sec$; F = the Faraday constant, 96500 coulomb $eq^{-1}$. By using Eqn. 5, an empirical correlation may be obtained between the cathodic input current and the concentration of dissolved hydrogen, $C_o$, just at the surface. The diffusivity value shown in Table (1) was used for these calculations.

It is seen from Table 3 that a hydrogen concentration of about 0.5 ppm is sufficient to cause embrittlement in quenched and tempered 4340 steel.

4. Scanning Electron fractrography of hydrogen embrittled 4340 steel

Hydrogen induced fracture in 4340 steel samples quenched from 1600°F and tempered at 450°F was studied by scanning electron microscopy. The fracture surface of a notched sheet specimen broken by tensile loading in air shows a large number of dimples formed by microvoid coalescence, indicating that fracture occurred in a ductile manner. By way of contrast, fracture surfaces of similar specimens hydrogen charged from the side opposite to the notch and fractured by tensile loading are totally different. Immediately beneath the notch is a region of predominantly intergrannular failure. At the hydrogen input side there is a region of ductile failure caused by shearing of the specimen due to overload. In the predominantly intergrannular fracture near the notch, a large number of secondary cracks along austentic grain boundaries is also observed. Some of the austentic grain boundary faces show ductile dimples and tear ridges, suggesting local plastic deformation at the grain boundary area (26).

## Table 3

Hydrogen concentration at the root of the notch at fracture

Material: 4340 quenched from 1600°F and tempered at 450°F for 2 hours.

Charging conditions: One sided charging from 0.2 N NaOH, 22°C

$\frac{C^{\sigma}}{C^{\circ}}$ (from Eq.4) = 1.81

$\sigma$ = maximum tensile stress at notch root = 324 KSI

D = (in eq.5) = $2.2 \times 10^{-7}$ $cm^2/sec.$

| charging current density ($mA/cm^2$) | $C_o$ (mole H/cc) | Time to failure (sec.) | $C^{\circ}_{\text{notch root}}$ (moleH/cc) | Applied stress (Ksi) | $C_{\text{notch root}}$ moleH/cc | PPM |
|---|---|---|---|---|---|---|
| 0.125 | $2.04 \times 10^{-6}$ | 1380 | $1.19 \times 10^{-6}$ | 128 | $2.16 \times 10^{-6}$ | 0.55 |
| 0.250 | $3.22 \times 10^{-6}$ | 864 | $1.22 \times 10^{-6}$ | 98.5 | $2.21 \times 10^{-6}$ | 0.56 |

$C_o$ = Hydrogen concentration at the charging side

$C^{\circ}_{\text{notch root}}$ = Hydrogen concentration at the notch root at the time of failure, neglecting the effect of stress.

$C^{\sigma}_{\text{notch root}}$ = Hydrogen concentration at the notch root at the time of failure when the effective stress at the area is $\sigma$.

Ductile failure regions are also observed adjacent to intergranular regions. Similar features have been previously observed (27) in hydrogen induced failure of steels.

Of significance is the fact that ductile failure (due to overload) takes place in the region which has the highest concentration of hydrogen, having propagated from the notch side as an intergranular fracture mode starting at the stress concentration region.

## 5. CONCLUSIONS

5.1 Hydrogen permeation characteristics of 4340 steel strongly depend upon the strength level of the steel. Hydrogen diffusivity of the steel decreases from $7.5 \times 10^{-6}$ $cm^2/sec$ for the annealed (84KSI) state to $0.22 \times 10^{-6}$ $cm^2/sec$ for the quenched and tempered (270KSI) state. A concurrent increase in hydrogen solubility with strength level is also observed. The forty-fold increase in hydrogen solubility observed in quenched and tempered steel as compared to the annealed material is attributed to trapping in the highly defective structure of the quenched and tempered steel.

5.2 Hydrogen charging has relatively little effect on the shape of the tensile stress-strain curve of annealed 4340 steel. The elastic region of the curve as well as the yield strength are unaffected. Hydrogen charging however reduces the elongation at fracture of the annealed steel. Fracture in hydrogen charged specimens occurred in a completely ductile fashion. No embrittlement was observed in the annealed material.

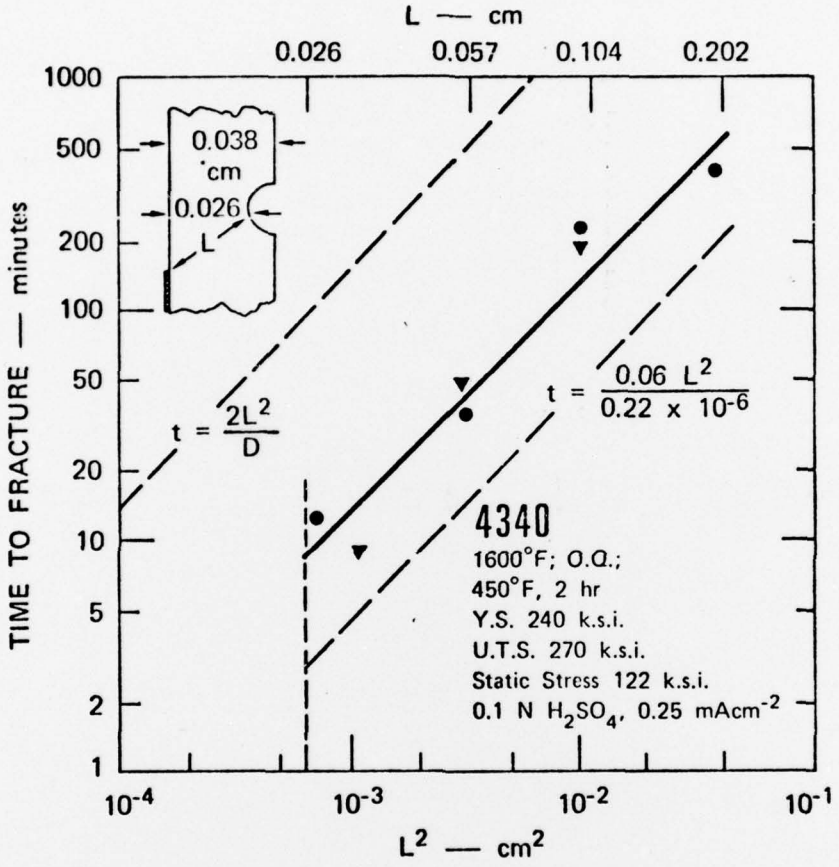
L — cm
0.026
0.057
0.104
0.202
1000
500
200
100
50
20
10
5
2
1
TIME TO FRACTURE — minutes
0.038 cm
0.026
L
$t = \frac{2L^2}{D}$
$t = \frac{0.06\ L^2}{0.22 \times 10^{-6}}$
4340
1600°F; O.Q.;
450°F, 2 hr
Y.S. 240 k.s.i.
U.T.S. 270 k.s.i.
Static Stress 122 k.s.i.
0.1 N $H_2SO_4$, 0.25 $mAcm^{-2}$
$10^{-4}$
$10^{-3}$
$10^{-2}$
$10^{-1}$
$L^2$ — $cm^2$

Figure 1

5.3 Electrolytic hydrogen charging severely embrittles quenched and tempered 4340 steel (270KSI). Hydrogen induces failure in notched specimens of this material at stress levels less than half the yield stress. The fracture mode is also altered by hydrogen charging. Whereas a specimen tested in air failed in a ductile fashion, hydrogen charged specimens failed by intergranular brittle fracture.

5.4 In static fatigue tests on quenched and tempered steels it was observed that the failure time is directly proportional to the square of the distance through which hydrogen has to travel to reach the root of the notch from an inlet position. Thus, diffusion dependence of hydrogen embrittlement is experimentally brought out.

5.5 The critical hydrogen concentration needed to produce embrittlement in quenched and tempered 4340 steel was found to be of the order of 0.5 ppm.

## 6. REFERENCES


1. A.R. Troiano, Trans. ASM, 52, 54 (1960).

2. B.E. Wilde, Corrosion, 27, 326 (1971).

3. I.M. Bernstein, Mater.Sci.Engg., 6, 1 (1970).

4. E.A. Steigerwald, F.W. Schaller, A.R. Troiano, Trans.AIME, 218, 832 (1960).

5. R.P. Frohmberg, W.J. Barnett, A.R. Troiano, Trans.ASM, 47, 892 (1955).

6. E.A. Steigerwald, F.W. Schaller, A.R. Troiano, Trans.AIME, 215, 1048 (1959).

7. R.A. Oriani, Ber.Bunsenges., Physik. Chem., 76, 848 (1972).

8. H.H. Johnson, J.G. Morlet, A.R. Troiano, Trans.AIME, 212, 528 (1958).

9. M.A.V. Devanathan, Z.O.J. Stachurski, Proc.Roy.Soc.A270, 90 (1962).

10. J. McBreon, L. Nanis, W. Beck, J.Electrochem.Soc., 113, 1218 (1966).

11. L. Nanis, TKG Namboodhiri, J.Electrochem.Soc., 119, 691 (1972).

12. TKG Namboodhiri, L. Nanis, Hydrogen permeation and embrittlement in ferrous materials, Technical Report, UPH2-004, Office of Naval Research, NR .036-077, November 1972.

13. B.G. Reisdorf, Trans.AIME, 227, 1334 (1963).

14. N.A. Tiner, C.B. Gilpin, Corrosion, 22, 271 (1966).

15. D.A. Vaughan, D.I. Phalan, Stress corrosion testing, ASTM, STP 425, 209 (1967).

16. J.G. Mailet, H.H. Johnson, A.R. Troiano, J.Iron and Steel Institute, 37 (May 1958).

17. F. Dekazinczy, J.Iron and Steel Institute (London) 177, 85 (1954).

18. N.J. Petch, P. Stables, Nature, 169, 842 (1952).

19. A.R. Troiano, Hydrogen in Steel, British Iron and Steel Institute, 1 (1961).

20. L.S. Darken, Trans. AIME, 180, 430 (1949).

21. P.S.H. Henry, Proc.RoyalSoc. (London), 171A, 231 (1939).

22. R.A. Oriani, Trans. AIME, 236, 1368 (1966).

23. C.E. Inglis, Trans.Inst.Naval Arch., 55, 219 (1913).

24. J.A. Hendrikson, D.S. Wood, D.S. Clark, Trans. ASM, 50, 656 (1958).

25. J. O'M. Bockris, W. Beck, M.A. Genshaw, P.K. Subramanian, F.S. Williams, Acta Met., 19, 1209 (1971).

26. C.D. Beachem, Trans. ASME, 87, series D, 229 (1965).

27. A. Phillips, V. Kerlins, B.V. Whiteson, Electron Fractography Handbook, Technical Report ML-TDR-64-416, 1965, AD 612 912.